Optical Properties of Zn(O,S) Thin Films Deposited by RF Sputtering, Atomic Layer Deposition, and Chemical Bath Deposition

Preprint

Jian Li
National Renewable Energy Laboratory and *Colorado School of Mines*

Stephen Glynn, Steven Christensen, Jonathan Mann, Bobby To, Kannan Ramanathan, Rommel Noufi, and Dean Levi
National Renewable Energy Laboratory

Thomas E. Furtak
Colorado School of Mines

Available electronically at http://www.osti.gov/bridge

Available for a processing fee to U.S. Department of Energy
and its contractors, in paper, from:

U.S. Department of Energy
Office of Scientific and Technical Information

P.O. Box 62
Oak Ridge, TN 37831-0062
phone: 865.576.8401
fax: 865.576.5728
email: mailto:reports@adonis.osti.gov

Available for sale to the public, in paper, from:

U.S. Department of Commerce
National Technical Information Service
5285 Port Royal Road
Springfield, VA 22161
phone: 800.553.6847
fax: 703.605.6900
email: orders@ntis.fedworld.gov
online ordering: http://www.ntis.gov/help/ordermethods.aspx

Cover Photos: (left to right) PIX 16416, PIX 17423, PIX 16560, PIX 17613, PIX 17436, PIX 17721

Printed on paper containing at least 50% wastepaper, including 10% post consumer waste.

Optical Properties of Zn(O,S) Thin Films Deposited by RF Sputtering, Atomic Layer Deposition, and Chemical Bath Deposition

Jian Li[1,2], Stephen Glynn[1], Steven Christensen[1], Jonathan Mann[1], Bobby To[1], Kannan Ramanathan[1], Rommel Noufi[1], Thomas E. Furtak[2], and Dean Levi[1]

[1]National Renewable Energy Laboratory, Golden, CO 80401, USA
[2]Department of Physics, Colorado School of Mines, Golden, CO 80401, USA

Abstract — **Zn(O,S) thin films 27 – 100 nm thick were deposited on glass or Cu(In$_x$Ga$_{1-x}$)Se$_2$/Molybdenum/glass with RF sputtering, atomic layer deposition, and chemical bath deposition. The complex dielectric functions ε of these films were extracted by spectroscopic ellipsometry and transmission analyses. It is found that ε varies on a large scale, indicative of significant variations in the films' chemical and physical properties, with the growth methods and deposition parameters. By fitting the ε spectra based on the parabolic band approximation, the E$_0$ critical point energies and broadening parameters were quantified to provide insights on the band gap, defect density, and phase segregation.**

Index Terms — **dielectric constant, ellipsometry, nanocrystals, photovoltaic cells, thin films, wide band gap semiconductors, Zinc compounds.**

I. INTRODUCTION

ZnS is an attractive material for photovoltaic (PV) applications. Potentially, it can replace the widely used n-type junction partner CdS with the advantages of wider band gaps and low toxicity. As-grown ZnS thin films could contain a significant amount of oxygen [1,2], which was found, i.e., in this study, to be beneficial to cell performance in some cases. Therefore, Zn(O,S) thin films with or without intentional addition of oxygen are of broad interest to PV technologies.

However, properties of near-intrinsic ZnS films vary with growth conditions, and the introduction of oxygen makes such variations substantially more complicated. In the Zn(O,S) thickness regime that is suitable for fabricating solar cells, usually ≤ 50 nm, many characterization techniques, such as x-ray diffraction and band gap calculation from transmission and reflectance, cannot provide reliable information due to the small thickness, whereas ellipsometry is a powerful tool owning to its high sensitivity to the film thickness and optical properties [3], both of which are important for understanding the materials properties and optimizing the cell performance.

II. EXPERIMENTAL DETAILS

Zn(O,S) thin films were deposited on glass substrate by RF sputtering and atomic layer deposition (ALD), and on Cu(In$_x$Ga$_{1-x}$)Se$_2$/Mo/glass by chemical bath deposition (CBD). For RF sputtering, the key process variables include: 1. deposition temperature T in the range of 20 – 200°C; 2. Ar pressure p_{Ar} in the range of 4 – 16 mTorr; 3. O$_2$/[O$_2$+Ar] flow ratio in the range of 0 – 10%; 4. target power P in the range of 100 – 200 watts. The baseline sputtering parameters are: T=20°C, p_{Ar}=16 mTorr, P=200 watts, and O$_2$/[O$_2$+Ar]=0. For ALD performed with diethylzinc and [H$_2$S+H$_2$O], the key process variables include: 1. T; 2. the H$_2$O/H$_2$S pulse ratio. For CBD using an aqueous solution containing zinc sulfate (16.3 mM), thiourea (0.6 M), and ammonia (1.8 M), the key process variable was the bath temperature in the range of 60-85°C.

Spectroscopic ellipsometry (SE) and normal incidence transmission measurements were performed using a rotating compensator ellipsometer. For sputtered and ALD films, an SE methodology was adopted from that established in our previous works [4]. Both the film side and through-glass SE were performed at multiple angles of incidence (AOI), using a pair of focusing optics. For CBD films, only the film side measurements were performed at multiple AOIs, without the focusing optics.

III. RESULTS AND DISCUSSIONS

A. SE and transmission analyses

The ellipsometric angles (ψ, Δ) are defined as: tan(ψ)exp(iΔ)≡r_p/r_s, where r_p and r_s are the complex amplitude reflection ratio for the p- and s- polarized incidence light, respectively [3]. In the analyses of the SE and transmission data, each Zn(O,S) film was assumed to have a "bulk" layer and a surface over-layer. This was found to be necessary in order to obtain a reasonable fit to the SE data measured on both sides of the sample and the transmission simultaneously, especially in the spectral region near the band gap. Figure 1 demonstrates the experimental data and the model fit for the sample sputtered with the baseline parameters. The analysis of Fig. 1 returns a bulk layer thickness of 43.2 ± 0.1 nm, a surface over-layer thickness of 6.7 ± 0.1 nm, and the optical properties of the ("bulk") Zn(O,S) film to be discussed in the following subsections.
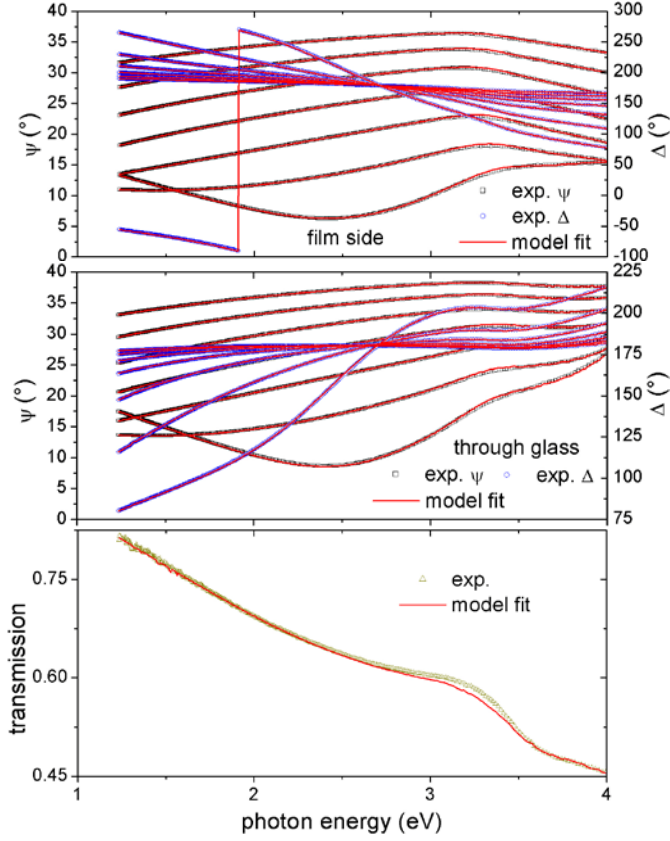
Fig. 1.   The experimental SE and transmission data, and the model fit for the Zn(O,S) sample sputtered with the baseline parameters.

B. RF Sputtering

The extracted complex dielectric functions $\varepsilon=\varepsilon_1+i\varepsilon_2$ of selected sputtered Zn(O,S) films are compared in Fig. 2. In the spectral range of $1.0 - 4.0$ eV, the dominant critical point (CP) feature in ε is the direct band gap transition E_0 [5]. To deduce the E_0 CP parameters, the second derivative spectra $d^2\varepsilon/dE^2$ were fit to an expression based on a parabolic band approximation and Lorentzian broadening:

$$\varepsilon(E_0) = A_0[\exp(i\phi_0)][E_0 - E - i(\Gamma_0/2)]^{\mu_0} \qquad (1)$$

where A_0, E_0, Γ_0, μ_0, and ϕ_0 are the amplitude, transition energy (also the fundamental band gap E_g), broadening parameter, exponent, and phase, respectively, of the E_0 CP [5]. As an example, the fit to the $d^2\varepsilon/dE^2$ spectra of the P=200 watts sample in Fig. 2(e) is shown in Fig. 2(f).

Theoretically, Γ_0 is related to the mean free path λ of excited carriers through the equation:

$$\Gamma_0 = \Gamma_{b0} + (h\upsilon_{g0}/\lambda) \qquad (2)$$

where Γ_{b0} is the broadening parameter of the single crystal (with a perfect lattice), h is the Planck constant, and υ_{g0} is the group speed of excited carriers associated with the E_0 transition [6]. Therefore, if defects scattering is the dominant mechanism that reduces λ, then Γ_0 is indicative of the average defect density; if grain boundary is the dominant scattering source, then Γ_0 is indicative of the average grain size [6].
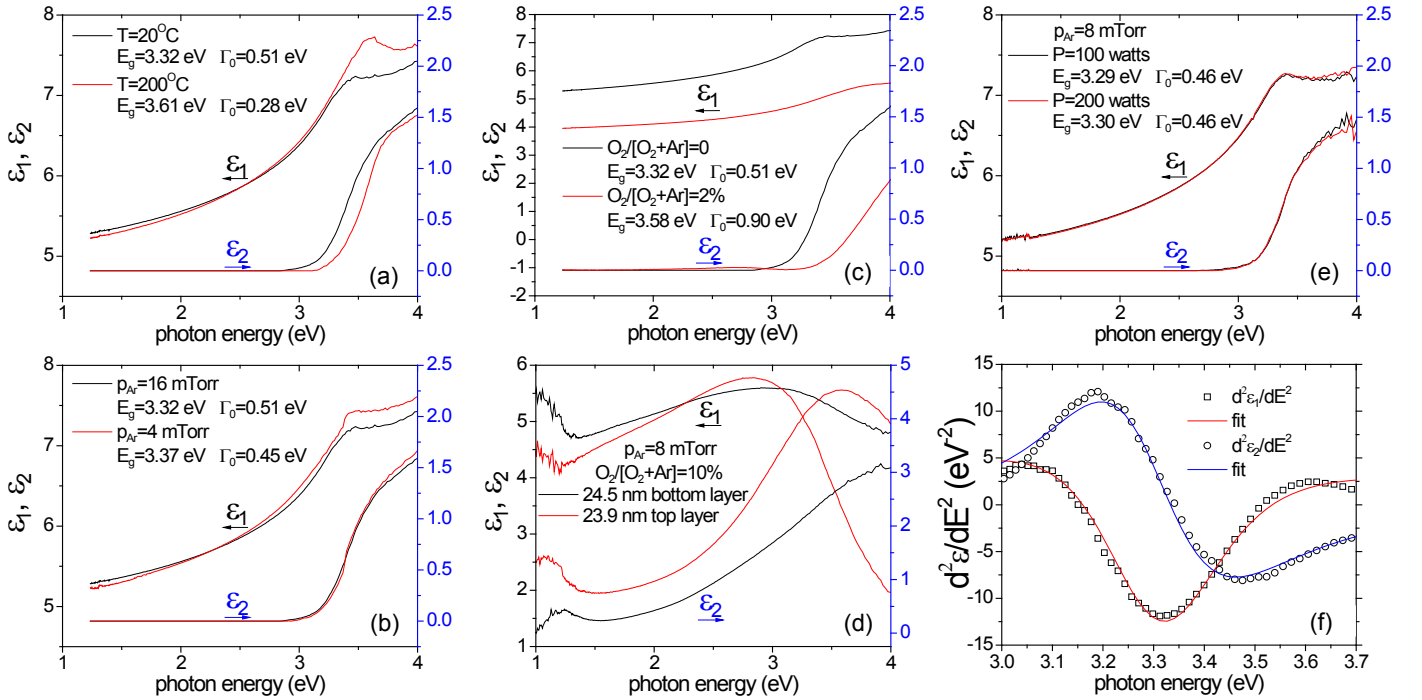

Fig. 2   (a) – (e): comparison of the $\varepsilon=\varepsilon_1+i\varepsilon_2$ spectra of the Zn(O,S) thin films RF sputtered under the specified conditions and otherwise identical baseline parameters; (f): $d^2\varepsilon/dE^2$ spectra of the P=200 watts sample in Fig. 2(e) and the fit based on Eq. (1). The deduced E_0 critical point energy E_g and the broadening parameter Γ_0 are also displayed in the relevant panels.
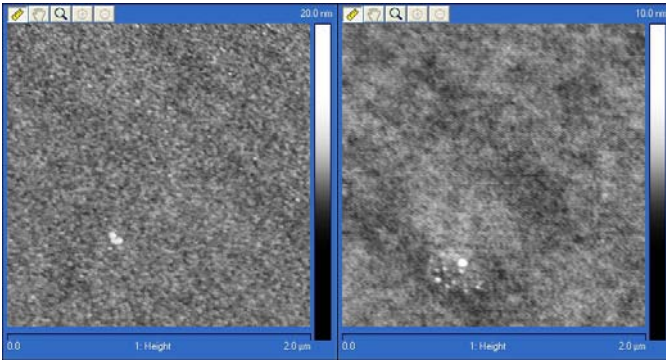
Fig. 3 Atomic force microscopy (AFM) images of the two Zn(O,S) films in Fig. 2(b). The left panel corresponds to the 16 mTorr film and the right panel corresponds to the 4 mTorr film.

Information from Fig. 2 includes the following.

2(a). Higher T decreases the defect density, possibly by increasing the grain size. Higher T also increases E_g, possibly by reducing the near-gap defect states.

2(b). Lower p_{Ar} decreases the defect density, possibly by increasing the grain size. Although this effect is not as clear as higher T in Fig. 2(a), it is consistent with the atomic force microscopy (AFM) images shown in Fig. 3.

2(c). The introduction of 2% O_2 flow significantly decreases the index of refraction n and increases E_g of the Zn(O,S) film. The lower n is consistent with adding O into ZnS, as n of ZnO is significantly lower than that of ZnS. However, a higher E_g is opposite the expectation of adding O into ZnS. One possible reason for increased E_g is the quantum confinement effect for nano-sized or amorphous grains with very small λ, consistent with the observed very large Γ_0 value.

2(d). If O_2 flow was further increased to 10%, the film became absorbing and hence not suitable as the buffer layer. SE + transmission analysis indicates that the film can be approximately divided into two layers with similar thicknesses. Their ε have a main CP feature near 3.0 eV, close to the E_g of ZnO. Another CP feature near 1.0 eV, however, is not present in the ε of any other samples in this study. The spectral range of this CP feature resembles that of the interband transition in single crystal Zn [7], indicating the existence of metallic Zn throughout the film. It is also clear that the main CP features in the bottom layer are broader as well as blue shifted compared to the top layer. A possible reason is the smaller grains in the bottom layer that broaden the CP according to Eq. (2) and at the same time blue shift the CP energies due to the quantum confinement effect.

2(e). P does not have a clear effect on the film properties.

C. Atomic Layer Deposition

The ε spectra of selected ALD Zn(O,S) films are compared in Fig. 4. Information can be drawn as follows.

4(a,b). In the range of 120°C ≤ T ≤ 200°C, there is a weak increase of E_g with increasing T. The trend in Γ_0, however, is not clear. There may exist an intermediate T around 150°C, at which the grain size is the smallest.
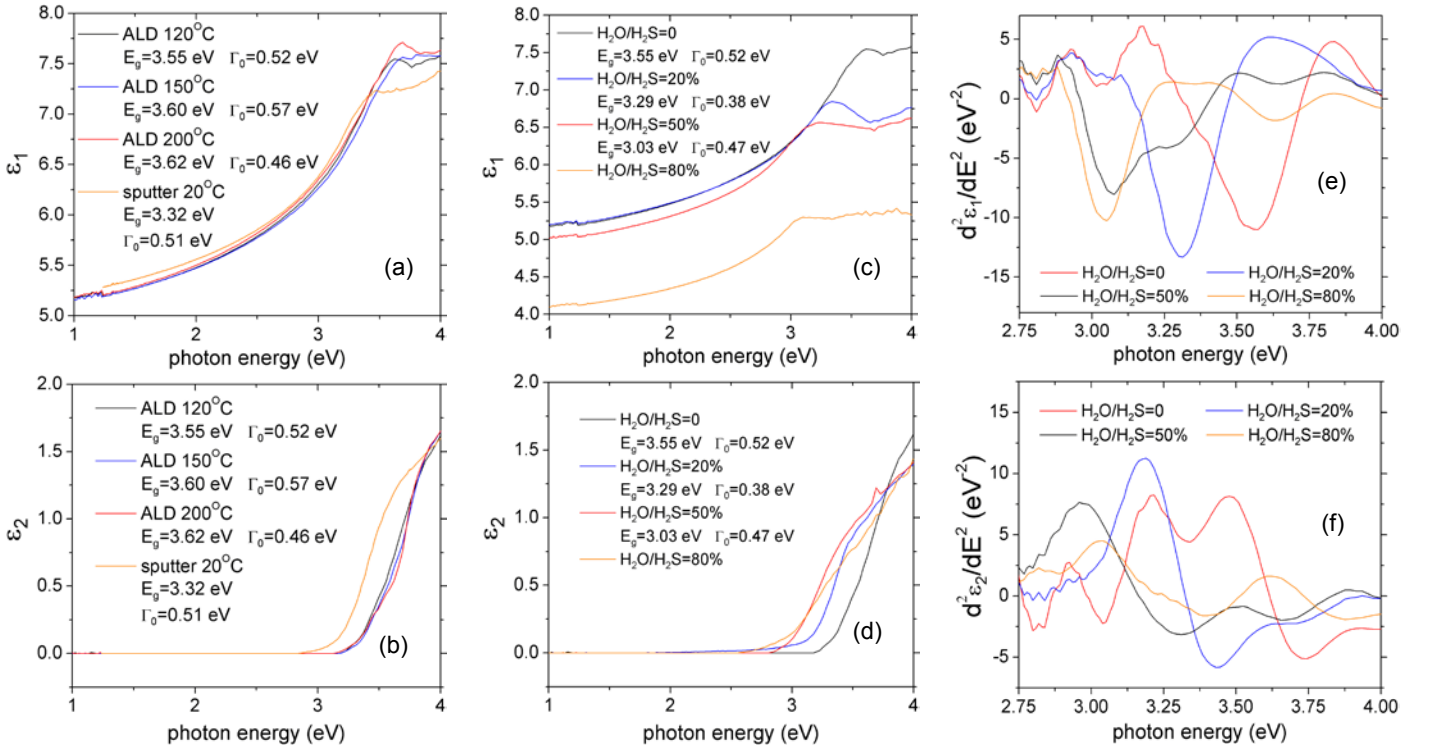

Fig. 4 (a) – (d): comparison of the dielectric functions ε of the Zn(O,S) thin films deposited by atomic layer deposition (ALD) under the shown conditions; (e) and (f): second derivative spectra for the films in (c) and (d).

4(c,d). In the range of $H_2O/H_2S \leq 50\%$, E_g decreases significantly, from that of ZnS toward that of ZnO, with increasing H_2O. At $H_2O/H_2S=80\%$, there is a ZnS-ZnO phase segregation, indicated by the two, instead of one, CP features in ε, one corresponding to ZnO and the other to ZnS. This is even clearer in the $d^2\varepsilon/dE^2$ spectra shown in Figs. 4(e) and 4(f), where the $H_2O/H_2S \leq 20\%$ films have a dominant peak and the $H_2O/H_2S=80\%$ film has two isolated peaks. The $H_2O/H_2S=50\%$ film appears to be at the onset of the phase segregation.

D. Chemical Bath Deposition

In this study, CBD films make excellent solar cells, with performances significantly better than cells with sputtered or ALD Zn(O,S), approaching the performance of cells with CdS. The ε spectra of two CBD Zn(O,S) films are compared in Fig. 5, together with the T=120°C ALD film with no H_2O. Some distinctive characteristics can be seen for the CBD films.

1. High E_g. Although X-ray photoelectron spectroscopy indicates that there is more O than S in the CBD films, their band gaps are the highest among all the films in this study.

2. Low index of refraction. N of the CBD films are ~ 20% less than that of the ALD film, even lower than pure ZnO, indicating porous structure. One immediate impact of low n on the cell fabrication is the necessary modification to the anti-reflection design. This topic will be discussed in detail in another IEEE-PVSC-38 paper.

3. Long absorption tail below the band gap. This indicates the existence of a significant amount of states within the gap.
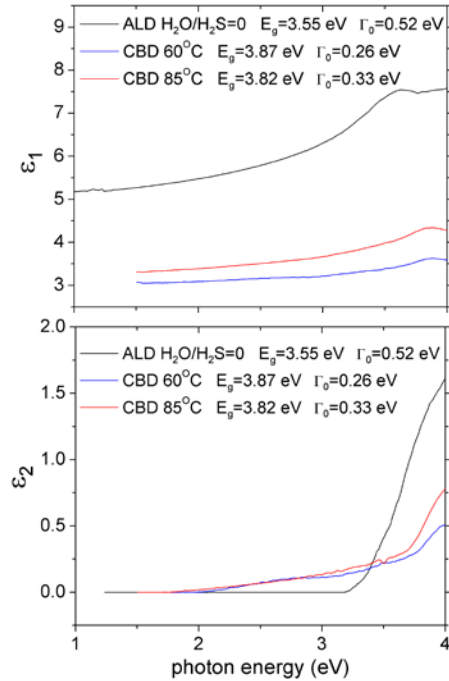
REFERENCES

[1] J. M. Blackmore, G. W. Blackmore, O. D. Dosser, and M. J. Slater, "The chemistry of the growth of ZnS deposited by r.f. sputtering onto cadmium stannate II: The bulk", *Thin Solid Films*, vol. 192 (2), pp. 321-334, 1990.

[2] T. Nakada, M. Mizutani, Y. Hagiwara, and A. Kunioka, "High-efficiency Cu(In,Ga)Se2 thin-film solar cells with a CBD-ZnS buffer layer", *Solar Energy Materials and Solar Cells*, vol. 67 (1-4), pp. 255–260, 2001.

[3] H. G. Tompkins and E. A. Irene (Editors), *Handbook of Ellipsometry*, Norwich NY, William Andrew Publishing, 2005.

[4] J. Li, H. Du, J. Yarbrough, A. Norman, K. Jones, G. Teeter, F. L. Terry, and D. Levi, "Spectral optical properties of Cu_2ZnSnS_4 thin film between 0.73 and 6.5 eV", *Optics Express*, vol. 20 (S2), pp. A327-A332, 2012.

[5] R. W. Collins and A. S. Ferlauto, "Optical Physics of Materials" in *Handbook of Ellipsometry*, chap. 2, edited by H. G. Tompkins and E. A. Irene, Norwich NY, William Andrew Publishing, 2005.

[6] G. F. Feng and R. Zallen, "Optical properties of ion-implanted GaAs: The observation of finite-size effects in GaAs microcrystals", *Phys. Rev. B*, vol. 40, pp. 1064-1073, 1989.

[7] R. H. W. Graves and A. P. Lenham, "Interband Absorption in Single Crystals of Mg, Zn, and Cd at 295°K and 82°K", *Journal Of The Optical Society Of America*, vol. 58 (1), pp. 126 – 129, 1968.

Fig. 5   Comparison of the ε spectra of the Zn(O,S) thin films deposited by chemical bath deposition (CBD) under the shown conditions and the ALD film with $H_2O/H_2S=0$ in Figs. 4(c) and 4(d).